Estuarine, Coastal and Shelf Science 208 (2018) 23–35

Contents lists available at ScienceDirect

Estuarine, Coastal and Shelf Science

journal homepage: www.elsevier.com/locate/ecss

Mangrove carbon assessment tool: Model development and sensitivity analysis

Zhaohua Dai[a,d,*], Carl C. Trettin[a], Steve Frolking[b], Richard A. Birdsey[c]

[a] Center for Forested Wetlands Research, USDA Forest Service, Cordesville, SC USA
[b] Earth System Research Center, University of New Hampshire, Durham, NH USA
[c] Woods Hole Research Center, Falmouth, MA USA
[d] School of Forest Resources and Environmental Science, Michigan Tech University, Houghton, MI USA

ARTICLE INFO

Keywords:
MCAT-DNDC
Marine wetland
Dissolved carbon
Particulate organic carbon
Burial carbon
CH_4
Blue carbon

ABSTRACT

It is important to have the capability to assess carbon (C) dynamics in mangrove forests and estimate their role in mitigating climate change because of their high carbon density, the threats to their integrity from land-use change and sea-level rise, and functional linkages of the many goods and services. A process-based model for mangroves was developed by integrating new features with existing biogeochemical processes in Forest-DNDC for simulating C sequestration and turnover in mangrove ecosystems. The new model is used to assess (1) the dynamics of C, nitrogen and phosphorous in mangrove ecosystems, including above-and below-ground C in saline wetlands, (2) the impacts of ecological drivers, including climate, soil nitrogen and phosphorous deficit and salt stress, on mangrove production, (3) the production of methane, and aerobic and anaerobic oxidation of methane with sulfate, nitrate and nitrite reductions, (4) the contributions of dissolved inorganic C (DIC), dissolved organic C (DOC), particulate organic C (POC) and burial C (BC) to blue C, and (5) impacts of natural and anthropogenic disturbances on C sequestration in mangrove ecosystems. Model sensitivity analysis showed that C sequestration in mangrove ecosystems was highly sensitive to multiple ecological factors, including climate, soil phosphorus, salinity and sulfate, as well as latitude. The responses of different C components to these factors were distinct. The responses of gross and net primary productivity and aboveground biomass to alterations of mean daily temperature (MDT) were quadratic, or increasing or decreasing non-linearly with an increment or decrement in MDT, but leaf production was linear. Similarly, other mangrove C components, such as BC, DIC, DOC and POC, respond substantially to variations of the ecological drivers. The combined effects of the driving factors are complex due to their intricate interactions. For example, while mangrove productivity is sensitive to available phosphorous, phosphorous cannot mitigate the stress imposed by high salinity. These results highlight the value of a tool to assess C dynamics in mangroves, especially for regional or large mangrove forests.

1. Introduction

Mangroves are widely recognized and valued for their ecological functions and socioeconomic values (Clough, 1998; Chen and Twilley, 1999; Alongi, 2009; Barr et al., 2012; Castaneda-Moya et al., 2013) because they provide a variety of goods and services and play an important role in the global C cycle. High rates of C sequestration and large accumulated C stocks are characteristics of mangroves, and are a foundation for mitigating climate change (Jennerjahn et al., 2017) and reducing damages of landward ecosystems in coastal areas threatened by tsunamis and hurricanes (Kathiresan and Rajendran, 2005; Alongi, 2008).

Mangroves not only accumulate C in woody biomass, but also bury C (BC) in sediments/soils (Matsui, 1998; Donato et al., 2011; Kauffman et al., 2011; Wang et al., 2013; Kauffman et al., 2014; Jones et al., 2014) and export DIC, DOC, and POC to oceanic deposition (Alongi, 2009, 2014; Dittmar et al., 2006). Mangroves are also a source of renewable resources for local communities (FAO, 1994). Their contributions to the global C cycle and mitigating climate change are substantially different from other terrestrial forests. However, mangroves are being rapidly depleted and degraded (FAO, 2007) due to increasing pressures from climate change and growing populations. Accordingly, understanding C dynamics in mangrove forests is fundamental to assess their contribution to mitigating climate change and inform mangrove management and MRV (Monitoring, Reporting and Verification) for REDD+ (Reducing emissions from deforestation and forest

* Corresponding author. Center for Forested Wetlands Research, USDA Forest Service, Cordesville, SC USA.
E-mail addresses: mcatdndc2015@gmail.com, zdai@fs.fed.us (Z. Dai).

https://doi.org/10.1016/j.ecss.2018.04.035
Received 27 April 2017; Received in revised form 6 March 2018; Accepted 27 April 2018
Available online 01 May 2018

degradation, plus conserving forests and promoting sustainable forest management).

Mangroves are dynamic and their production varies widely due to differences in ecological factors, including species composition (Alongi, 2009; Rahman et al., 2015), geographic location (Bouillon et al., 2008; Alongi, 2014), salinity (Naidoo, 1987; Ball and Pidsley, 1995; Galvan-Ampudia and Testerink, 2011), topographic gradient (Alongi, 2014), and nutrient status (Lin and Sternberg, 1992; Twilley and Day, 1999; Liang et al., 2008). While mangrove carbon stocks have been characterized amongst a wide variety of mangrove types and regional eco-environmental conditions, existing inventories are insufficient to understand long-term C, nitrogen (N) and phosphorous (P) dynamics in mangrove forests, especially for large regions where limitations in personnel, equipment, funds and complex environmental conditions prevent comprehensive inventories. Mechanistic computer models, which are developed from expert knowledge and observations, are an important additional tool for understanding mangrove ecosystems.

There are several models with capability to assess C dynamics in mangrove ecosystems (Chen and Twilley, 1998; Luo et al., 2010; Barr et al., 2013a; Hutchison et al., 2013; Grueters et al., 2014; Jardine and Siikamaki, 2014; Bukoski et al., 2017), however, most of these models are empirical and not spatially-explicit. Except for the model modified from Biome-BGC (Luo et al., 2010), which can be used to estimate more than two mangrove C components, the other models can only be used to assess either biomass and/or NPP or soil C in mangrove ecosystems. There are also two models with functionalities that can be utilized to assess effects of disturbances on mangroves and estimate recovery after disturbances (Rideout et al., 2013; Mukherjee et al., 2014). However, there isn't a model that can simultaneously estimate dynamics of several important mangrove C components, including aboveground and belowground biomass, soil C pool, and aquatic C (DIC, DOC and POC) and gaseous C (CH_4 and CO_2) fluxes, and that can also access the effects of multiple disturbances on mangroves.

There are substantial differences in ecological drivers, such as climate, soil and hydrology, as well as species composition that influence C sequestration in mangroves. Accordingly, a spatially-explicit process-based assessment tool is needed to estimate spatial dynamics of two important C processes in mangrove ecosystems, the contribution of mangroves to blue C[1] and mitigating climate change, and to assess the impacts of natural and anthropogenic disturbances on C sequestration in mangrove ecosystems.

We have developed a process-based model for mangroves by integrating features unique to mangroves within the biogeochemical process based model Forest-DNDC for simulating C dynamics. The following presents (1) the spatially-explicit, process-based mangrove carbon assessment tool, and (2) results from sensitivity analyses for the environmental factors used as model inputs that may substantially impact C sequestration in mangrove ecosystems. Vegetation and soil characteristics at a site in the Everglades National Park (ENP) in Florida of USA (Castaneda-Moya et al., 2013) were used as the basis of the sensitivity analysis because this site has been widely studied with respect to biomass estimate, soil analysis and water table observations. The analysis involves quantifying the sensitivities of gross primary productivity (GPP), net primary productivity (NPP), aboveground biomass (AGB), BC, DOC, DIC, and POC, as well as CH_4 flux and heterotrophic soil respiration (Rh) to climate, latitude, salt stress (salinity) and P deficiency, and combined effect of soil salinity and P as well as the impact of combined climate and latitude on C sequestration in mangrove ecosystems.

[1] Blue carbon is the carbon captured by oceans and coastal ecosystems.

2. Modeling methods

2.1. Model framework

The model, MCAT-DNDC (Mangrove-Carbon-Assessment-Tool-DeNitrification-DeComposition), was constructed by integrating existing biogeochemical processes of Forest-DNDC (Li et al., 2000) with new components that consider processes specific to mangroves. Forest-DNDC (FDNDC) has been used to assess C dynamics in forested uplands and freshwater wetlands (Zhang et al., 2002; Li et al., 2004; Cui et al., 2005; Dai et al., 2012). FDNDC is process-based, and used to simulate forest growth and above- and below-ground C and N dynamics in forest ecosystems, including trace gas emissions, based on the balance of water, light, and nutrition in forest ecosystems (Li et al., 2000; Stange et al., 2000; Miehle et al., 2006). The model integrates photosynthesis, decomposition, nitrification-denitrification, carbon storage and consumption, and hydrothermal balance in forest ecosystems. The vegetation is divided into three layers: overstory, understory, and ground. The vegetation of each layer is simulated based on competition for energy and nutrients. This model has been tested and used for estimating greenhouse gas (GHG) from forested upland and freshwater wetland ecosystems and assessing C sequestration in forests in a wide range of climatic regions, from boreal to tropical (Stange et al., 2000; Zhang et al., 2002; Li et al., 2004; Dai et al., 2014).

The processes in FDNDC were modified to estimate C dynamics in mangroves because the physiological mechanisms and rooting environment of mangroves are substantially different from those of terrestrial forests. The MCAT-DNDC estimates C, N and P dynamics in saline wetlands (Fig. 1), and predicts mangrove growth and degradation, C accumulation in aboveground and belowground biomass, litter production and decomposition and organic C accumulation in soil/sediment, as well as the effects of N and P deficit and salt stress on above- and below-ground biomass; and MCAT-DNDC assesses the anaerobic oxidation of methane (AOM) via sulfate, nitrate and nitrite reduction, as well as production of DIC, DOC, POC and BC and their contributions to blue C; the model can also be used to assess the impacts of natural and anthropogenic disturbances, including insects, storms, fires and harvesting, on mangroves.

To better accommodate the spatial heterogeneity in biophysical and biogeochemical conditions in mangrove ecosystems, MCAT-DNDC is designed to explicitly represent spatial complexities in hydrogeological and climatic characteristics, and soil and vegetation types at different scales that are flexible from a single soil-plant profile to a large region consisted of various geographical mosaics. A polygon-based spatial dataset joined vegetation, soil, climate and geographical gradient is used for the model set-up (Dai et al., 2017), i.e., each polygon contains the information needed to assess C, N and P dynamics in mangrove ecosystems. The model runs daily on a daily time-step for all processes and polygons are processed sequentially.

2.2. Carbon accumulation and consumption

Rates of accumulation and consumption of C in mangrove ecosystems are principally dependent on ecological drivers (Fig. 1). The main drivers are vegetation, soils/sediments, hydrology regulated by climate and tides, disturbance, and incoming radiation impacted by climatic conditions. Plants use light energy to assimilate atmospheric CO_2 by photosynthetic process to accumulate C in ecosystems. Primary productivity is related to the accumulation rate of biomass. Gross primary productivity (GPP) is used to represent the capability of plants assimilating CO_2. However, plants release CO_2 too because of respiration needed for growth and maintenance of the plant. Accordingly, net primary productivity (NPP) is used to quantitatively reflect C accumulation in the plant systems, or

$$NPP = GPP - R_p \quad (1)$$

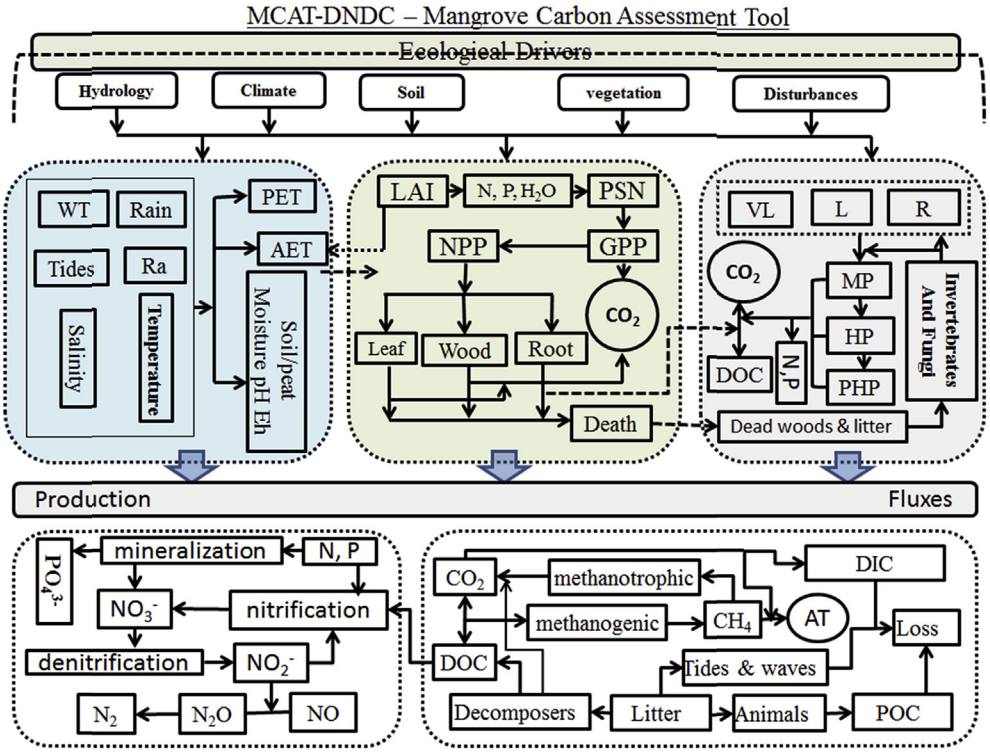

Fig. 1. The framework of MCAT-DNDC. WT: water table; Ra: radiation; PET: potential evapotranspiration; AET: estimated actual evapotranspiration; PSN: photosynthesis; NPP: net primary production; GPP: gross primary production; Death: including fallen leaf and dead woods; VL: very labile organic matter; L: labile organic matter; R: resistant organic matter; MP: mineral C pool; HP: humus pool; PHP: positive pool; DIC: dissolved inorganic C; DOC: dissolved organic C; AT: atmosphere; POC: particle organic C.

where R_p represents the plant respiration, which is:

$$R_p = R_l + R_w + R_r \tag{2}$$

where R_l is leaf respiration; R_w and R_r are aboveground woody tissue and root respiration, respectively.

Similar to Forest-DNDC (Li et al., 2000; Dai et al., 2012), MCAT-DNDC uses a multi-layer canopy to simulate photosynthesis such that GPP is the sum of photosynthetic C of all canopy layers:

$$GPP = \beta \times f(t, m) \times \sum FPAR_i \times LAI_i \tag{3}$$

where β is the photosynthetic rate, 5–25 μmol CO_2 m^{-2} s^{-1} for different species (Alongi, 2009); $f(t, m)$ is a coefficient of temperature and moisture regulated by climate and hydrology; $FPAR_i$ is available PAR (photosynthetically active radiation) at ith layer of the canopy depth starting from the top, and $FPAR_0$ is the PAR above the canopy that is related to geographical location; LAI_i is the leaf area index at the ith layer, calculated from leaf weight (see Eq. (7)) divided by specific leaf weight (SLW, g m^{-2}).

Net primary production (NPP) reflects the net C sequestration or accumulation (see Eq. (1)) within the ecosystem over a specified period. However, C loss from organic matter decomposition (e.g., heterotrophic respiration R_h) must be also considered for C balance in ecosystems. Net ecosystem exchange (NEE) is, thus, used to determine the net exchange of C between the ecosystem and the atmosphere (Eqn. (4)) (Kirschbaum et al., 2001)

$$NEE = NPP - R_h \tag{4}$$

where R_h is heterotrophic respiration, representing land surface gaseous C flux excluding root respiration, only CO_2 resulted from dead organic matter decomposition.

NEP (net ecosystem productivity) is similar to NEE, which is used to estimate C accumulation in ecosystem. However, NEE does not consider non-gaseous C loss, thus, NEE may be larger than the value of NEP (Lovett et al., 2006) because

$$NEE = NEP + \Delta DIC + \Delta DOC + \Delta POC + \Delta O_X \tag{5}$$

where ΔDIC, ΔDOC and ΔPOC are the parts of DIC, DOC and POC losses from mangrove ecosystems to oceanic/aquatic ecosystems, respectively. These three components are important for estimating the roles of mangrove ecosystems in mitigating climate change. ΔO_X is the C loss to or obtaining from other natural factors, such as methane release from or uptake by soils/sediments.

Natural and anthropogenic disturbances impact C sequestration in mangroves. Accordingly, net biome productivity (NBP) is used to assess how much C can accumulate in the ecosystem over a specified period (Eq. (6)).

$$NBP = NEP - \sum D_i \tag{6}$$

where D_i is C removal from the ecosystems by ith disturbance factor. The factors considered in our model framework include harvest, insects, fires, and storms.

2.3. Salt stress

Salt stress influences mangrove productivity (Parida and Das, 2005). A common response to salt stress is that the leaf surface expansion is reduced, thereby reducing photosynthesis, which in turn reduces mangrove production (Ball and Farquhar, 1984; Ball and Pidsley, 1995; Takemura et al., 2000; Parida et al., 2004; Suarez and Medina, 2005; Nguyen et al., 2015). The leaf production of mangroves and the impact of salt stress on the production are estimated in MCAT-DNDC as:

$$W_i = W_{i-1} + \alpha_i \times f_{tm} \times f_s \tag{7}$$

where W_i and W_{i-1} are leaf mass at the *i*th and *i-1*th time steps; i = 1, 2, 3, …, n; W_0 = 0 when i = 0; α_i is the correspondent growth rate of the leaf at the *i*th time step; f_{tm} is the coefficient of temperature and moisture, which are regulated by climate, hydrology and physical soil properties; f_s is salinity coefficient, given by

$$f_s = e^{-\omega s} \tag{8}$$

where ω is a coefficient, 0.0225, and s is salinity (ppt, parts per thousand).

2.4. Phosphorus

Many studies have concluded that phosphorus (P) deficiency in mangroves can influence productivity (Alongi, 2009). Phosphorus concentration in near shore marine sediments typically ranges between 8 and 108 μmol g^{-1} (Filippelli, 1997). The ratio of organic P to inorganic P in oceanic sediments varies largely based on P species in oceanic sediments (Baturin, 2003). Dissolved P in pore water of oceanic sediments is between < 0.01 and 40 mg l^{-1}, dissolved organic P in oceanic water is about 1–40 μg l^{-1}. Dissolved inorganic P is mainly available for plants, occurs in oceanic surface water as HPO_4^{2-} (about 87%) and PO_4^{3-} (12%) (Baturin, 2003). However, the impact of P on plant growth is complicated because P availability for plants is influenced by many factors, including ionic concentration of Ca, Mg and Na, and pH and fungi (Grattan and Grieve, 1999). The interaction between P and salinity makes the effect of P on mangrove growth even more complex (Chapin, 1980; Clarkson, 1985; Bolan, 1991; Grattan and Grieve, 1992; Schachtman et al., 1998; Dakora and Phillips, 2002).

The rate of P uptake by plants is the key index to estimate the effect of P on mangrove production. A Michaelis-Menten equation (Clarkson, 1985) was used to estimate P uptake by plant as follows

$$P_u = \frac{P_{max} \times (C_s - C_{min})}{K_m + (C_s - C_{min})} \quad (9)$$

where P_u is P uptake by plants; P_{max} is maximum P uptake while P is adequate; C_s is the P concentration in the rhizosphere; C_{min} is the minimum concentration in the rhizosphere at the level that P uptake by plant is 0, or $P_u = 0$; K_m is equal to $(C_s - C_{min})$ while $P_u = 0.5 \times P_{max}$. We assumed $C_{min} = 0$, and P_{max}= P demand amount by mangroves at daily base when P is enough. Accordingly, K_m is a constant (mg P) under a specific environment, 0.1 mg P for initial input. C_s varies in soils, depending on many factors, including (1) total P in soils, (2) organic P mineralization (Froelich, 1988; Li et al., 1992; Follmi, 1996), (3) fixation of phosphorus (Tiessen et al., 1984; Van der Molen, 1991; Ingall et al., 1993; Filippelli and Delaney, 1996; Filippelli, 1997; Bridgham et al., 1998), and (4) equilibrium between dissolved P ions and phosphates (Atlas et al., 1976; Johansson and Wedborg, 1979; Froelich, 1988; Burton and Walter, 1990; Vazquez et al., 2000).

2.5. Dissolved inorganic carbon

DIC consists of dissolved gaseous CO_2 ($CO_{2(aq)}$), HCO_3^- and CO_3^{2-} (DOE, 1994), i.e.,

$$DIC = CO_{2(aq)} + HCO_3^- + CO_3^{2-} \quad (10)$$

We assume that dissolved CO_2 in the surface water of mangroves has been reached under equilibrium with atmospheric conditions and the solution content of carbonate and sulfate. Concentration of dissolved DIC should closely correlate to the partial pressure of CO_2 (Raymond et al., 2000). Accordingly, DIC generation in mangrove systems is mainly controlled by organic matter decomposition (OMD), mangrove root respiration (R_r, see Eq. (2)) and the hydrogeological characteristics. The concentrations, diffusion and flux of gaseous CO_2, $CO_{2(aq)}$, HCO_3^- and CO_3^{2-} are calculated at each time step based on the changing hydrology and climate, and CO_2 released from OMD and R_r to pore water in mangrove systems.

2.6. Production and anaerobic oxidation of methane

Production and emission of CH_4 in rice paddies and forested freshwater wetlands have been described in previous versions of DNDC (Li et al., 1992, 2000; Zhang et al., 2002; Cui et al., 2005; Li, 2007), which focus on (1) the effects of sulfate reduction and oxides of iron and manganese on the redox potential that regulates CH_4 production, (2) gaseous diffusion in soils, and (3) impacts of water depth and plants on CH_4 fluxes under freshwater conditions. This functionality has been modified for MCAT-DNDC to include the impact of tides on sulfate concentration in pore and surface water in mangroves (see below), which influences CH_4 production and emission.

Anaerobic oxidation of methane (AOM) was not in Forest-DNDC because changes in sulfate, nitrate and nitrite concentration were either small or not frequent in freshwater wetlands, thus, their reductions were assumed to mainly influence Redox potential that regulates CH_4 production in freshwater wetland ecosystems. However, studies have shown that AOM with sulfate, nitrate and nitrite reductions may play an important role in CH_4 flux from saline tidal wetlands (Joye et al., 2004; Shima and Thauer, 2005; Raghoebarsing et al., 2006; Ettwig et al., 2010; Thauer, 2011; Joye, 2012; Haroon et al., 2013) because of frequently varying concentrations of these compounds, especially given sulfate's high concentration in seawater. Accordingly, AOM with nitrate, nitrite and sulfate reduction in mangrove ecosystems is more complicated due to tides that make the concentration of these substances in the water dynamic in mangrove wetlands, which impacts Redox potential and methane production and oxidation in mangrove systems. The dynamic concentration is estimated as

$$[A]_i = [A]_{i-1} + \Delta[A] \quad (11)$$

where $[A]_i$ and $[A]_{i-1}$ are sulfate, nitrate and nitrite concentration in mangrove systems at the ith and i-1^{th} time; and $\Delta[A]$ is added by tides or consumed by reductions, and the sign is positive for addition and negative for reduction; and when $i = 0$, $[A]_i$ is the initialized value, equal to the measured or estimated concentration in pore water in target study mangroves. The impact of these acidic substances on Redox potential regulating CH_4 production is simulated firstly with the variable concentrations, and then AOM is estimated.

AOM by sulfate reduction may also produce more DIC in mangrove ecosystems (Caldwell et al., 2008; Milucka et al., 2012) as follows

$$CH_{4(aq)} + SO_4^{2-} \rightarrow HS^- + HCO_3^- + H_2O \quad (12)$$

AOM with nitrate and nitrite reductions resulted in reducing CH_4 flux from mangrove wetlands (Ettwig et al., 2010; Haroon et al., 2013; Green-Saxena et al., 2014) are

$$CH_{4(aq)} + 4NO_3^- \rightarrow CO_2 + 4NO_2^- + 2H_2O, \quad (13)$$

and

$$3CH_{4(aq)} + 6NO_2^- \rightarrow 3CO_2 + 3N_2 + 6H_2O \quad (14)$$

Dissolved CH_4 was calculated based on its stability and solubility in marine sediments (Sun and Duan, 2007) to estimate AOM with sulfate, nitrate and nitrite reductions. We assumed that principal gases in the pore water in mangrove systems are CO_2 and CH_4, other gases are not considered.

3. Model parameterization for sensitive analysis

MCAT-DNDC was parameterized to analyze the sensitivity of the mangrove C cycle to ecological drivers (Table 1). The vegetation and soil characteristics from an Everglades National Park (ENP) site in Florida (Fig. 2) were used as the basis of this analysis because it has well documented measures of biomass, NPP based on eddy covariance, soil characterization and water table within the mangroves (Barr et al., 2006, 2010, 2013b; Twilley, 1985; Chen and Twilley, 1999; Romigh et al., 2006; Castaneda-Moya et al., 2013).

Studies have shown that biomass and litter production of mangroves are related to latitude (Bouillon et al., 2008; Alongi, 2009). In order to analyze this effect and the combining effect of temperature and latitude, 16 locations, including ENP, were selected along Atlantic coast of USA and Caribbean coast of Mexico, between about 15.06° and 34.97° N latitude (Fig. 2).

Climatic data was obtained from the Daymet database (Thornton et al., 2012; http://daymet.ornl.gov/index.html) for the 16 sites,

Table 1
Initialization of key parameters for MCAT-DNDC.

Item	Value	Item	Value
β, photosynthetic rate (μmol m^{-2} s^{-1})	16	K_b, light attenuation constant	0.58
Pc, photosynthetic capacity (nmol s^{-1} g^{-1} N)	68	ω, salt stress coefficient	0.0225
To, optimal photosynthetic temperature (°C)	25	K_m, P deficit coefficient	0.1
Tn, minimum photosynthetic temperature (°C)	2	L_r, leaf retention years	1.33
Tx, maximum photosynthetic temperature (°C)	45	$L_{C/N}$, C/N ratio in leaf	35
Ka, half saturation constant, μ mol m^{-2} s^{-1}	150	$L_{N/P}$, N/P ratio in leaf	10
Nc, initial N concentration in foliage (%)	1.25	$W_{C/N}$, C/N ratio in wood	200
Wu, water demand for producing a unit of biomass	30.9	$W_{N/P}$, N/P ratio in wood	16
Cs, critical concentration of P uptake by plants	0	specific leaf weight (g m^{-2})	110
α, coefficient of leaf growth potential	0.01	Organic C in organic layer (%)	PB
Daily minimum temperature (°C)	PB[a]	Organic C in mineral soils (%)	PB
Daily maximum temperature (°C)	PB	P in organic layer (g kg^{-1})	PB
Daily precipitation (mm)	PB	P in mineral layer (g kg^{-1})	PB
Latitude (decimal)	PB	Sulfate in pore water (mol l^{-1})	PB
Maximum tidal height (cm)	PB	Daily water table (cm)	PB
Minimum tidal height (cm)	PB		

[a] PB, the value is plot based.

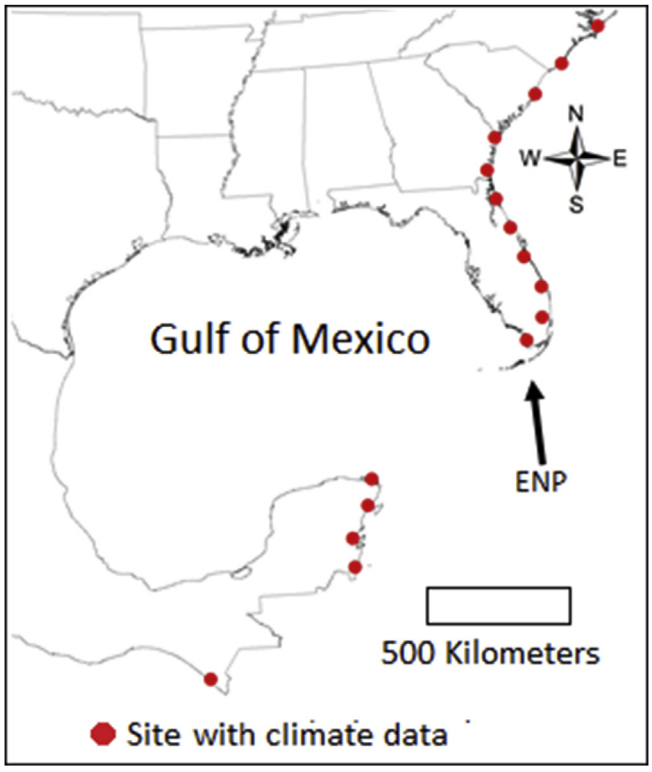

Fig. 2. Climate data at sites (red points) along Atlantic coast of USA and Caribbean of Mexico used for model sensitivity analysis; ENP, Everglades National Park in Florida, USA. (For interpretation of the references to colour in this figure legend, the reader is referred to the Web version of this article.)

including daily minimum and maximum temperature and daily precipitation, and used to analyze the sensitivity of mangrove C to temperature and precipitation and the combined effect of climate and latitude.

To analyze mangrove C sensitivity to salinity, sulfate, P, and the combined impact of soil salinity and P deficiency, the model was run using different salinity, and P and sulfate concentrations (Table 2); inter-combinations of salinity and P were used to analyze their combined impacts on C dynamics in mangrove ecosystems. These inter-combinations created two combined effects of salinity and phosphorus (SP, in which both P and salinity increased from low to high values, and PS, in which P decreased from high to low while salinity increased from low to high; see Table 2).

Water table (WT) depth is an important attribute that influences C dynamics in mangroves. Unfortunately, WT data were not available for all sites used in this study. Accordingly, we created a WT dataset based on the pattern of WT in 2002 at the ENP site in Florida (Castaneda-Moya et al., 2013); this dataset was used for all simulations. This meant that changes in sea level were not considered. Other assumptions were: (1) all locations/plots used for sensitivity analysis were fully forested, or canopy cover at these sites should be approximately 100% when mangroves are mature; (2) the land use at these points has been mangroves over hundreds of years, based on accumulated soil/sediment organic layer thickness that is over several meters at ENP (Castaneda-Moya et al., 2013); (3) current mangroves at all sites were naturally regenerated; (4) there were no disturbances following stand establishment, although this model contains functionality to estimate the effects of disturbances including fire, hurricane, insects and harvest. The simulation period was 200 years, beginning with natural stand regeneration. This time span was selected to accommodate assessment of C dynamics from stand development through maturity.

4. Statistical analysis

Univariate and multivariate linear and non-linear regressions were used to analyze the sensitivity for main eco-environmental drivers used as model inputs. The level of statistical significance was set to $\alpha = 0.02$ to determine whether C cycle components were sensitive to one or multiple eco-environmental factors, rather than $\alpha = 0.05$; accordingly, the use of "significant" or "significantly" indicates $P \leq 0.02$.

The average values were calculated for mature mangrove forests (stand age ≥20 years old), and standard deviation for the same period. Annual BC (cohort mass) was the difference between current and previous year. Annual aboveground net primary productivity (ANPP) was the sum of annual net increment in aboveground biomass and litter-fall, calculated as dry matter (Mg ha^{-1} yr^{-1}).

5. Results and discussion

5.1. Climatic factors

Leaf biomass (LPD), a surrogate for leaf area, significantly ($P < 0.001$) increased linearly with an increase in mean daily temperature (MDT) (Table 3a), at a rate of about 67 kg C ha^{-1} yr^{-1} per °C. Correspondingly, both GPP and NPP were sensitive to temperature, exhibiting different quadratic response functions to increased air temperature (Fig. 3, Table 3a). GPP tended to increase or decrease with a corresponding change in MDT between 18 and 24 °C. However, when MDT was over 25 °C, GPP did not increase substantially with an

Table 2
Various soil salinity and concentrations of P and sulfate, and different combinations of salinity and P used to analyze sensitivity of mangrove to these components.[a]

Factor $(P)_i$	Value (g kg^{-1})	Factor $(S)_i$	Value (ppt)	Factor PS_i	Value (g kg^{-1}/ppt)	Factor SP_i	Value (ppt/g kg^{-1})	Sulfate SF_i	Value (mol l^{-1})
P1	0.1	S1	5	PS1	2.0/5	SP1	5/0.1	SF1	0.175
P2	0.2	S2	10	PS2	1.7/10	SP2	10/0.2	SF2	0.350
P3	0.3	S3	15	PS3	1.4/15	SP3	15/0.3	SF3	0.524
P4	0.5	S4	20	PS4	0.8/20	SP4	20/0.5	SF4	0.699
P5	0.8	S5	25	PS5	0.5/30	SP5	30/0.8	SF5	1.049
P6	1.1	S6	30	PS6	0.3/40	SP6	40/1.4	SF6	1.398
P7	1.4	S7	40	PS7	0.2/50	SP7	50/1.7	SF7	1.748
P8	1.7	S8	50	PS8	0.1/60	SP8	60/2.0	SF8	2.098
P9	2.0	S9	60						

[a] P1 – P9, changes in soil phosphorus concentration (g P kg^{-1}); S1 – S9, changes in salinity (ppt); PS1 – PS8, phosphorus decrease companioned by an increase in salinity; SP1 – SP8, an increase in both salinity and phosphorus; SF1 – SF7, soils sulfate concentration; all other ecological drivers were as same as those at NEP.

Table 3a
Statistic results from Univariate linear and non-linear regressions for sensitivity analysis.[a]

Variables	*n*	R^2	Equation
LPD vs T	16	0.9944	$67.406 \times T + 2332.6$
LLT vs T	16	0.9944	$67.376 \times T + 2330.6$
AGB vs T	16	0.9869	$-0.231 \times T^2 + 12.322 \times T + 25.549$
GPP vs T	16	0.9368	$-7.055 \times T^2 + 349.0 \times T - 1498.0$
NPP vs T	16	0.9725	$-8.688 \times T^2 + 343.4 \times T - 1473.9$
BC vs T	16	0.9778	$6.188 \times T - 7.637$
DIC vs T	16	0.9457	$-0.612 \times T^2 + 24.194 \times T - 53.846$
DOC vs T	16	0.9651	$2.441 \times T + 36.73$
POC vs T	16	0.0624	$-0.4639 \times T + 98.535$
Rh vs T	16	0.9960	$-2.843 \times T^2 + 149.46 \times T - 566.96$
CH_4 vs T	16	0.9727	$1.1345 \times T - 3.0887$
ANPP vs T	16	0.9635	$0.234 \times T + 10.597$
TLT vs T	16	0.9844	$0.1071 \times T + 4.6583$
LPD vs L	16	0.9985	$-123.9 \times L + 5788.5$
LLT vs L	16	0.9985	$-122.86 \times L + 5741.2$
AGB vs L	16	0.9999	$0.0091 \times L^3 - 0.8018 \times L^2 + 2.263 \times L + 103.65$
GPP vs L	16	0.9999	$-1.1174 \times L^2 + 5.5864 \times L + 2282.2$
NPP vs L	16	0.9999	$0.0351 \times L^3 - 3.5069 \times L^2 + 15.686 \times L + 1014.8$
ANPP vs L	16	0.9968	$-0.4226 \times L + 20.866$
BC vs L	16	0.9974	$-1.2224 \times L + 49.917$
DIC vs L	16	0.9092	$-2.2234 \times L + 196.42$
DOC vs L	16	0.9984	$0.0084 \times L^3 - 0.6027 \times L^2 + 11.701 \times L + 22.325$
POC vs L	16	0.9995	$-2.7519 \times L + 130.71$
Rh vs L	16	0.9983	$-17.793 \times L + 980.8$
CH_4 vs L	16	0.9836	$-0.0404 \times L + 3.2095$
LPD vs S	9	0.9991	$-21.984 \times S + 3147.7$
LLT vs S	9	0.9989	$-21.716 \times S + 3119.9$
AGB vs S	9	0.9949	$-0.0035 \times S^2 - 0.6234 \times S + 109.02$
GPP vs S	9	0.9999	$-0.074 \times S^2 - 4.4779 \times S + 1864.1$
NPP vs S	9	0.9989	$-0.0379 \times S^2 - 3.045 \times S + 973.98$
ANPP vs S	9	0.9992	$-0.1015 \times S + 12.806$
BC vs S	9	0.9997	$0.0002 \times S^3 - 0.1043 \times S^2 + 2.2909 \times S + 9.3844$
DIC vs S	9	0.9996	$-0.0008 \times S^3 + 0.0437 \times S^2 - 1.0034 \times S + 154.01$
DOC vs S	9	0.9961	$0.0063 \times S^2 - 1.0878 \times S + 44.74$
POC vs S	9	0.9916	$-1.0795 \times S + 83.731$
Rh vs S	9	0.9949	$-0.1057 \times S^2 + 0.2963 \times S + 612.29$
LPD vs P	9	0.9979	$-194.32 \times P^4 + 1348.8 \times P^3 - 3586.7 \times P^2 + 4471.9 \times P + 539.97$
LLT vs P	9	0.9979	$-193.73 \times P^4 + 1343.8 \times P^3 - 3568.8 \times P^2 + 4441.5 \times P + 537.01$
AGB vs P	9	0.9991	$4.2376 \times P^4 - 14.995 \times P^3 - 18.133 \times P^2 + 113.24 \times P + 3.307$
GPP vs P	9	0.9985	$-210.13 \times P^4 + 1350.5 \times P^3 - 3154.7 \times P^2 + 3249.0 \times P + 467.62$
NPP vs P	9	0.9867	$-69.057 \times P^4 + 440.84 \times P^3 - 1051.3 \times P^2 + 1168.0 \times P + 377.56$
BC vs P	9	0.9979	$-8.4929 \times P^4 + 59.366 \times P^3 - 159.45 \times P^2 + 201.14 \times P + 4.334$
DIC vs P	9	0.9999	$25.954 \times P^5 - 203.11 \times P^4 + 613.06 \times P^3 - 894.73 \times P^2 + 637.15 \times P + 17.341$
DOC vs P	9	0.9975	$1.1092 \times P^3 - 11.737 \times P^2 + 33.731 \times P - 1.8159$
POC vs P	9	0.9982	$5.4663 \times P^3 - 36.204 \times P^2 + 78.845 \times P + 10.998$
Rh vs P	9	0.9971	$62.853 \times P^3 - 352.6 \times P^2 + 643.15 \times P + 60.863$
CH_4 vs P	9	0.9966	$0.3031 \times P^3 - 1.6673 \times P^2 + 2.964 \times P + 2.307$
ANPP vs P	9	0.9991	$1.0219 \times P^3 - 6.6933 \times P^2 + 14.384 \times P + 1.3175$

[a] T, temperature, °C; L, latitude, degree; S, salinity, ppt; P, soil phosphorous, g P kg^{-1}; *n*, number of samples; R^2, coefficient of determination, squared correlation coefficient; others, as same as those in text; LPD and LLT, kg C ha^{-1}; AGB and TLT, Mg C ha^{-1}; GPP, NPP, BC, DIC, DOC, POC and Rh, g C m^{-2}, respectively; ANPP, Mg dry matter per hectare; CH_4, mg CH_4 $m^{-2}d^{-1}$.

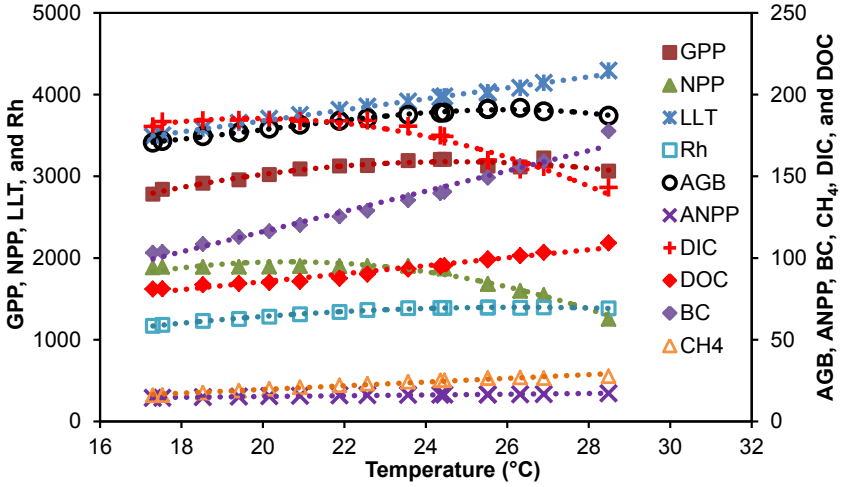

Fig. 3. Sensitivity of GPP, NPP, DIC, DOC, Rh and BC (g C m^{-2}), LLT (kg C ha^{-1}), AGB (Mg C ha^{-1}), ANPP (Mg dry matter ha^{-1}) and CH_4 (mg m^{-2} d^{-1}) to temperature (soil salinity and phosphorous, and hydrological conditions were the same as at the NEP plot in Florida, USA (Castaneda-Moya et al., 2013)); see Table 3a for correlative equations and the correlations to temperature (T).

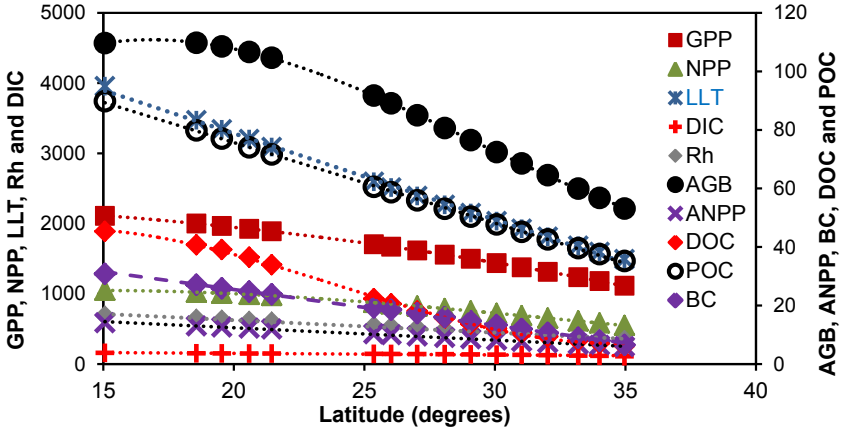

Fig. 4. Effect of latitude on AGB (Mg C ha^{-1}), ANPP (Mg dry matter ha^{-1}), GPP, NPP, BC, DIC, DOC, POC and Rh (g C m^{-2}), and LLT (kg C ha^{-1}), respectively (environmental conditions, except latitude, were the same as those at ENP in Florida, USA); see Table 3a for the correlative equations and correlations to latitude (L).

increment in MDT.

NPP increased with an increase in temperature when MDT ≤ 25 °C, but it reduced nonlinearly with an increase in temperature when MDT > 25 °C, because autotrophic respiration increases with an increase in temperature. Correspondingly, AGB exhibited a quadratic response to changes in MDT, it increased with an increment in MDT when MDT was ≤25 °C, and when MDT was over 25 °C, AGB did not increase with an increase in MDT, but it decreased little when MDT > 26 °C.

The responses of fluxes of DIC, DOC and POC, and BC and total litter (TLT, leaf + root + woody litter) to changes in MDT were different (Fig. 3, Table 3a). DIC was quadratic ($R^2 > 0.94$, $n = 16$), and BC, DOC and TLT were linear. BC, DOC and TLT increased substantially ($P < 0.001$) with an increase in temperature, at a rate of about 6.2, 2.4 and 10.7 g C m^{-2} yr^{-1} per °C, respectively. However, POC had only a minor change with an increase or decrease in temperature (by 0.464 g C m^{-2} yr^{-1} per °C) due to POC flux being regulated mainly by hydrology.

CO_2 flux from heterotrophic soil respiration (Rh) (Fig. 3) was strongly influenced by MDT ($R^2 = 0.996$, $n = 16$, $p < 0.001$). Its response to changes in temperature was quadratic, with an optimum at about 26 °C. When MDT was ≤26 °C, the flux increased substantially with an increase in temperature, but when MDT was over 26 °C, the flux increased little with an increase in temperature. CH_4 emission was also influenced by temperature, increasing approximately linearly below 25 °C, and with little sensitivity above 25 °C.

The results indicate that temperature can substantially affect C sequestration in mangrove ecosystems, including C accumulation in the mangrove forest and soil/sediment and C export to the ocean; and these results also indicate that the model simulates the effect of temperature on C storage in sediments and woody product, and loss C to atmosphere as CO_2 (Rh) and CH_4, and export C to aquatic ecosystems as DIC, DOC and POC.

C sequestration in mangrove ecosystems showed little sensitivity to precipitation ($P > 0.1$) within the precipitation range used in this study (1113–1966 mm y^{-1}). Accordingly, results related to the direct effect of precipitation on the dynamics of mangrove C are not reported, though the effect of precipitation on mangrove C sequestration may also be implicit in the latitudinal relationships with productivity (see below). There may be two principal reasons for the small effect of precipitation on mangrove C: first, the precipitation range we used (1113–1966 mm) may be over the threshold level of precipitation that can substantially influence C sequestration in mangroves (Osland et al., 2014); second, our assumption that the hydrological, vegetation and soil conditions for this analysis were the same as those at ENP in Florida (Fig. 1).

5.2. Geographical location

Bouillon et al. (2008) and Alongi (2009) suggest that leaf litter production (LLT) and AGB of mangroves are closely related to latitude, decreasing with an increase in latitude. Simulated results showed that LPD, LLT, GPP, NPP, AGB, BC and fluxes of DIC, DOC and POC decreased significantly ($P < 0.001$) with an increase in latitude (Fig. 4 and Table 3a). These variable responses to changes in geographical

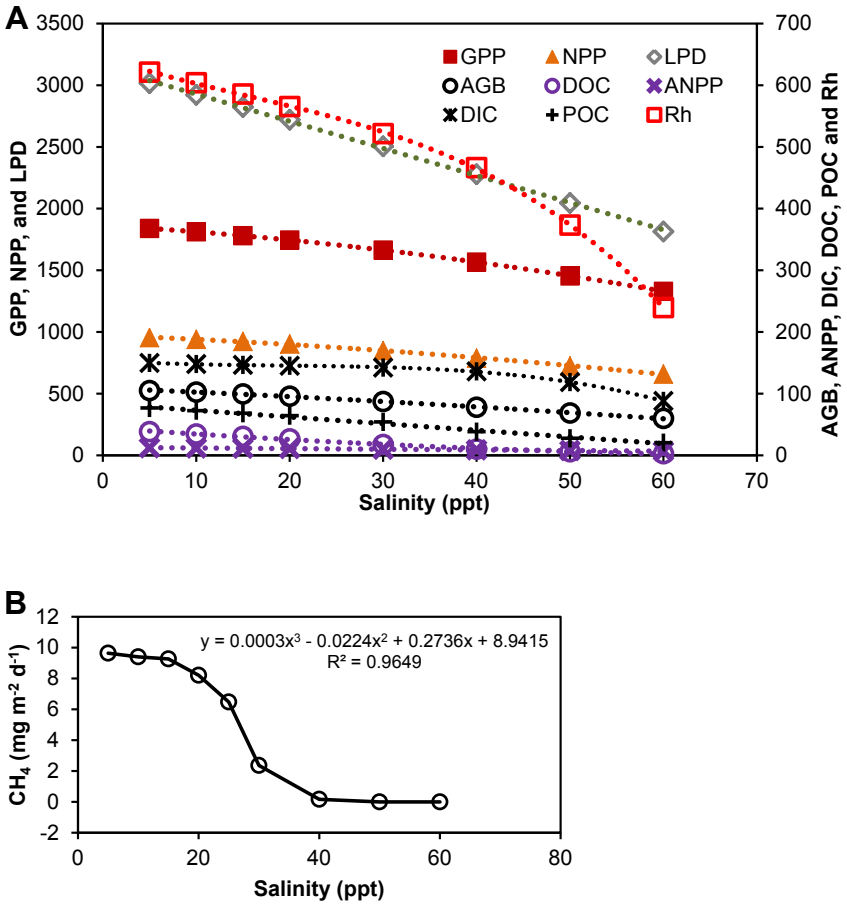

Fig. 5. (a). Impacts of soil salinity on LLT (kg C ha^{-1}), AGB (Mg C ha^{-1}), ANPP (Mg ha^{-1}), and GPP, NPP, DIC, DOC, POC, and Rh (g C m^{-2}) (other environmental conditions were the same as those at ENP in Florida, USA); see Table 3a for the correlative equations and the correlations to salinity (S). **(b)**. The effect of salinity on CH_4 (environmental conditions, except salinity, were the same as those at ENP in Florida, USA).

latitudes were either linear, quadratic or cubic polynomial ($P < 0.001$).

GPP, NPP and DOC significantly decreased nonlinearly with an increment in latitude although they could also be well correlated linearly to latitude ($R^2 = 0.9863$, 0.971 and 0.9786 for GPP, NPP and DOC, respectively, with $P \ll 0.001$), similar to the findings reported by Alongi (2009). Other mangrove C components, including ANPP, BC, CH_4, DIC, LLT, LPD, POC and Rh significantly decreased linearly with an increase in geographical latitude.

LPD and LLT decreased similarly, at a rate of approximately 123 kg C ha^{-1} yr^{-1} per degree latitude, because annual leaf regeneration and leaf fall are almost equal in a mature mangrove forest. Annual LLT from this study for the latitude range between 15° and 35° corresponds with the findings reported by Bouillon et al. (2008).

ANPP, BC, DIC and POC decreased linearly by about 0.42 Mg ha^{-1} yr^{-1} for ANPP and by 1.22, 2.22 and 2.75 g C m^{-2} yr^{-1} for BC, DIC and POC, respectively, with an increase in latitude. The responses of the soil-borne gaseous C fluxes, Rh and CH_4 to changes in latitude were linear. CH_4 flux decreased with an increase in latitude at a rate of about 14.7 mg CH_4 m^{-2} yr^{-1} per degree latitude, Rh flux decreased at a rate of about 17.8 g C m^{-2} yr^{-1} per degree latitude.

There was a significant linear relationship between biomass and latitude from this study ($R^2 = 0.9613$, $P < 0.001$) although AGB from this analysis did not increase with a decrease in latitude when latitude was lower than 17° (Fig. 4). For latitudes > 17°, the linear decrease in AGB of about 6.4 Mg ha^{-1} per degree increase in latitude is similar to the trend of 6.1 Mg ha^{-1} found by Alongi (2009).

5.3. Salt stress

Numerous studies have shown that salinity can influence C sequestration in mangrove ecosystems (Ball and Farquhar, 1984; Takemura et al., 2000; Parida et al., 2004; Suarez and Medina, 2005). The sensitivity analysis showed that annual mean LPD decreased linearly ($P < 0.01$) with an increase in salinity (Fig. 5a, Table 3a), at a rate of approximately 22.0 kg C ha^{-1} yr^{-1} per 1.0 ppt increase in salinity within the range of 5–60 ppt. The linear correlation between litter-fall and salinity is similar to that reported by Day et al. (1996). However, the effect of salinity on annual mean litter-fall from this study was about 149 kg dry mass ha^{-1} yr^{-1} per ppt within a salinity range of 5–60 ppt, about 7 kg dry matter more than the mean value reported by Day et al. (1996) for fringe and basin mangroves in Campeche, Mexico, with salinities of 40–80 ppt.

AGB, GPP and NPP decreased quadratically with an increase in salinity (Fig. 5a), while the increase or decrease in BC with an increment or decrement in salinity was cubic polynomial. POC decreased linearly with an increase in salinity at a rate of about 1.08 g C m^{-2} yr^{-1} per ppt; DOC and DIC decreased quadratically and cubically, respectively, with an increase in salinity (Fig. 5a). However, the response of CH_4 to salt stress was more complex (Fig. 5b). CH_4 flux decreased slowly with an increasing salinity at low values (< 20 ppt), but decreased sharply between 20 and 40 ppt, and the flux was approximately zero when salinity was ≥ 50 ppt.

These responses of mangrove C components to salt stress affirm that the salinity in mangrove wetlands is an important factor that can impact C accumulation in mangrove ecosystems, i.e., the higher salt stress, the less the C sequestration in mangroves, especially in mangrove biomass, but response of BC to salt stress is not consistent with those responses of other mangrove C components, which might be related to lowering organic matter decomposition due to high salinity.

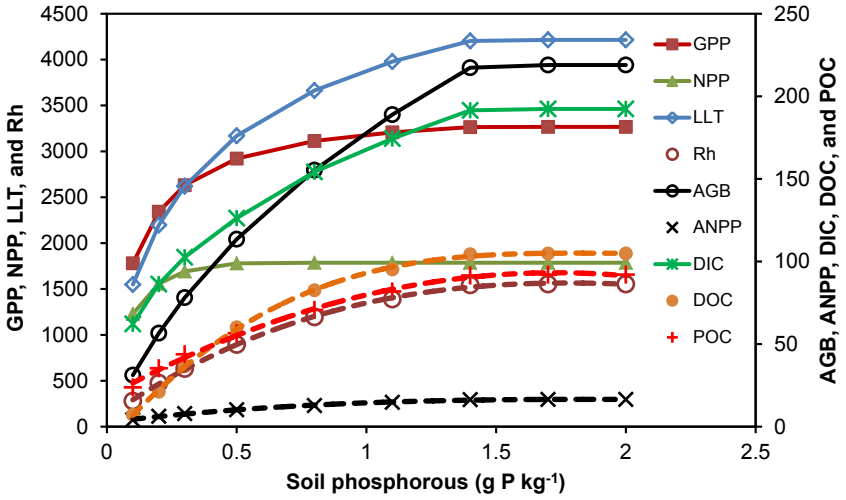

Fig. 6. Effect of P deficit on AGB (Mg C ha^{-1}), ANPP (Mg ha^{-1}), LLT (kg C ha^{-1}), and GPP, NPP, DIC, DOC, POC, and Rh (g C m^{-2}) (other environmental conditions are the same as those at ENP in Florida, USA); see Table 3a for the correlative equations and the correlations to phosphorus (P).

5.4. Phosphorus

Available soil P concentration for plants in mangrove ecosystems is considered as an important factor regulating mangrove production (Alongi, 2009). Similar to varied effects of salinity on C dynamics in mangroves, P strongly influences leaf production, and corresponding components of the C cycle (Fig. 6). Results from sensitivity analysis exhibited that the effect of soil P on GPP and NPP (Fig. 6) was large when soil P < 0.5 g kg^{-1}, but when P > 0.8 g kg^{-1}, GPP and NPP hardly increased with an increase in soil P. AGB, LLT and LPD increased non-linearly with an increase when P ≤ 1.4 g P kg^{-1}, and then hardly increased when P > 1.5. Accordingly, the equation used to describe the relationship between P and these three mangrove C components was complex (Table 3a). However, the response of ANPP to changes in

Table 3b
Statistic results from multivariate regression for sensitivity analysis.[a]

Variable	*n*	F	Significance	Equation
TLT	16	208.5	1.33E-10	4.411 − 0.030 × S + 1.054 × ln(P)
LPD	16	246.3	4.64E-11	2878.4 − 19.646 × S + 591.821 × ln(P)
LLT	16	245.0	4.79E-11	2853.2 − 19.422 × S + 585.742 × ln(P)
AGB	16	114.0	5.73E-09	92.799 − 0.549 × S + 29.557 × ln(P)
ANPP	16	149.5	1.07E-09	11.12 − 0.076 × S + 2.866 × ln(P)
GPP	16	138.9	1.69E-09	1838.2 − 10.548 × S + 321.15 × ln(P)
NPP	16	169.4	4.89E-10	958.3 − 5.706 × S + 138.96 × ln(P)
DIC	16	59.7	2.80E-07	224.588 − 1.85 × S + 37.779 × ln(P)
DOC	16	32.6	8.56E-06	28.36 − 0.38 × S + 6.693 × ln(P)
POC	16	53.7	5.19E-07	72.14 − 0.837 × S + 14.173 × ln(P)
BC	16	140.4	1.58E-09	59.19 − 0.346 × S + 19.393 × ln(P)
Rh	16	92.0	2.19E-08	460.533 − 3.811 × S + 101.99 × ln(P)
CH_4	16	30.3	1.27E-05	4.503 − 0.086 × S + 0.206 × ln(P)
GPP	16	6280.6	1.95E-19	146.181 × T − 0.274 × R − 1.192 × L
NPP	16	2706.9	2.57E-15	5.883 × T^2 − 327.522 × T − 0.090 × R − 9.615 × L^2 + 485.822 × L
ANPP	16	9781.7	1.37E-20	37.367 − 0.073 × T + 0.0002 × R − 0.828 × L
AGB	16	2334.4	7.28E-17	11.288 × T − 0.0004 × R − 3.000 × L
TLT	16	9863.1	1.30E-20	18.784 − 0.0425 × T + 0.00006 × R − 0.415 × L
LPD	16	3355.4	8.35E-18	11060.2 − 52.245 × T + 0.308 × R − 246.798 × L
DIC	16	1734.2	4.35E-16	5.837 × T + 0.033 × R − 0.089 × L
DOC	16	15524.8	8.57E-22	569.5 × T − 0.0077 × R − 2.057 × L
POC	16	418.6	2.10E-12	4.588 × T + 0.0094 × R − 1.287 × L
Rh	16	6011.2	2.54E-19	85.544 × T − 0.124 × R − 19.079 × L
CH_4	16	3633.6	5.18E-18	18.335 + 0.119 × T − 0.0003 × R − 0.461 × L
AGB	16	3775.5	5.55E-17	11.269 × T − 3.005 × L
GPP	16	32137.4	2.76E-22	49.626 × T + 166.86 × L + 0.545 × T^2 − 3.985 × L^2
NPP	16	3504.0	5.40E-17	−368.774 × T + 485.666 × L + 7.467 × T^2 − 9.299 × L^2
ANPP	16	2945.4	5.35E-18	0.919 × T − 0.264 × L
LPD	16	2054.3	5.53E-17	254.248 × T − 76.455 × L
LLT	16	2053.3	5.53E-17	254.087 × T − 76.415 × L
DIC	16	1749.6	1.56E-16	7.46 × T + 0.319 × L
DOC	16	11542.4	7.54E-22	6.158 × T − 2.152 × L
POC	16	644.0	9.95E-14	5.048 × T − 1.172 × L
BC	16	952.9	7.95E-15	10.569 × T − 4.085 × L
Rh	16	6316.9	3.78E-20	79.501 × T − 20.600 × L
CH4	16	4428.3	3.79E-19	0.588 × T − 0.188 × L
TLT	16	2865.4	6.39E-18	0.455 × T − 0.131 × L

[a] F, the statistic of F test; R, precipitation, mm; ln(P), natural logarithmic value of P; others, the same as those in Table 3a.

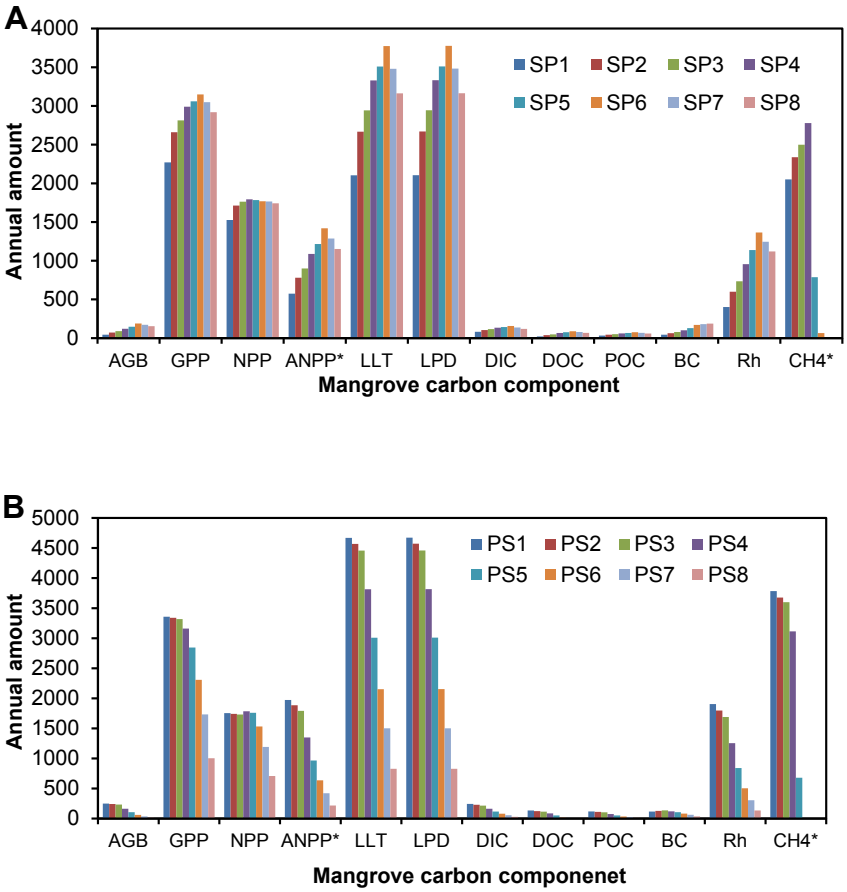

Fig. 7. (A). Combined effect of phosphorus-salinity (increase in both salinity and phosphorous, SP, see Table 2) on GPP, NPP, BC, DIC, DOC, POC, and Rh (g C m^{-2}), LLT and LPD (kg C ha^{-1}), AGB (Mg C ha^{-1}), CH_4* (mg CH_4 m^{-2}), and ANPP* (g dry matter m^{-2}); *: the units used for ANPP and CH_4 in this figure are different from those used in text and other figures; (Other environmental conditions are as same as those at ENP); see Table 3b for the correlative equations and the correlations to combined effects of phosphorus (P) and salinity (S). **(B).** Combined effect of phosphorus-salinity (dual pressure, PS in Table 2, or an increase in salinity and decrease in soil P) on GPP, NPP, BC, DIC, DOC, POC, and Rh (g C m^{-2}), LLT and LPD (kg C ha^{-1}), AGB (Mg C ha^{-1}), CH_4* (mg CH_4 m^{-2}), and ANPP* (g dry matter m^{-2}); *: the units used for ANPP and CH_4 in this figure are different from those used in text and other figures; (Other environmental conditions are as same as those at ENP); see Table 3b for the correlative equations and the correlation to the combined effects of salinity-phosphorus.

soil P was cubic polynomial, affirming that soil P can substantially influence mangrove production.

BC and fluxes of DIC, DOC and POC can be strongly sensitive to soil P content because P deficit can substantially impact the primary production of mangroves. Fig. 6 showed that the responses of DOC and POC to changes in soil P were cubic polynomial. They increased substantially with an increase in soil P when soil P $< 1.0\,g\,kg^{-1}$ ($P < 0.001$), and the increment became small when soil P $> 1.0\,g\,kg^{-1}$. However, the responses of BC and DIC to changes in soil P were high degree polynomial (Fig. 6, Table 3a), similar to the responses of AGB, GPP and NPP.

The fluxes of CH_4 and Rh can be influenced by soil P. The responses of these gaseous fluxes to soil P were cubic polynomial (Table 3a). Similar to DOC, when soil P was lower than $1.0\,g\,P\,kg^{-1}$, both fluxes of CH_4 and Rh increased largely with an increase in soil P, but the increment was small or unsubstantial when P $> 1.0\,g\,kg^{-1}$. The increment in DIC, DOC, POC and gaseous C fluxes with an increase in soil P exhibits that soil P content can substantially impact C dynamics in mangrove soil ecosystems.

5.5. Combined effect of salinity and phosphorus

Combined effects of salinity-phosphorus, SP and PS (see Table 2) on C sequestration in mangrove ecosystems are more complicated. Accordingly, the sensitivity of C sequestration in mangrove ecosystems to these complex effects was analyzed. Results from multivariate regression analysis (Table 3b) indicated that SP and PS substantially impacted C sequestration in mangrove ecosystems.

The multivariate effects of salinity and phosphorous on twelve mangrove C components were different from the individual impacts of salinity or P on these variables. In the SP case, the responses of these mangrove elements to increases in both salinity and P were divergent. AGB, GPP, ANPP, LLT, LPD and Rh increased with an increment in both salinity and P when salinity ≤ 40 ppt and P $= 1.4\,g\,kg^{-1}$, and they decreased with an increase in both salinity and P when salinity > 40 ppt, although P concentration was higher (Fig. 7a). The impact of SP on DIC, DOC and POC was similar to the effect on AGB. This combined impact on NPP and BC was smaller than or similar to that on other mangrove C components. CH_4 flux increased substantially with an increment in both salinity and P when salinity was < 20 ppt and P $< 0.5\,g\,kg^{-1}$, and then it decreased with an increment in both salinity and P when salinity > 20 ppt. Mangrove C cycling responds strongly and negatively to a combined increase in both salt stress and P deficit (Fig. 7b), particularly when salinity was ≥ 15 ppt and P was $\leq 1.4\,g\,kg^{-1}$.

This sensitivity analysis shows that both salinity and P are important factors influencing C sequestration in mangroves. High P cannot offset the effect of high salt stress although C sequestration in mangroves can substantially increase with an increment in P when salinity < 50 ppt; and dual pressure from high salinity and P deficiency can impede C sequestration in mangroves.

5.6. Combining climate with latitude

Assessment of the mangrove C balance for the 16 locations (Fig. 1) showed that the combined impact of latitude and climate was completely different from their individual effects, especially from the independent impacts of temperature and latitude. Result from single factor sensitivity analysis showed that AGB might increase or decrease by about 2.0 Mg C ha^{-1} with a decrease or increment in temperature of 1 °C (Fig. 3 and Table 3a) and by about 3.6 Mg C ha^{-1} with a decrease or increment in geographical latitude per degree when latitude $> 18°$ (Fig. 4 and Table 3a). However, the combined effect showed that AGB might only decrement at a rate of about 3.0 Mg C ha^{-1} per degree latitude with an

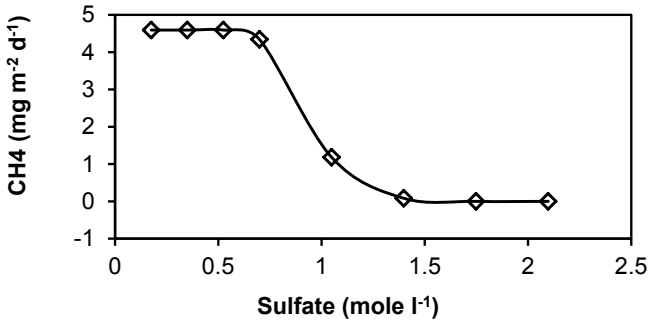

Fig. 8. Effect of sulfate on methane flux (Other environmental conditions are as same as those at ENP).

increase in latitude (Table 3b) within the same latitude range for single factor analysis, but the impact of temperature under this combined effect became larger than that from individual influence factor.

Similarly, the responses of other mangrove C components to this combined effect were different from their responses to single factors. The responses of GPP and NPP to changes in latitude became larger under the combined effect than their responses to changes in single factors, and their responses to temperature became smaller.

Comparing of the combined effects of latitude and climate with and without precipitation showed that precipitation has a small impact mangrove C. LPD and LLT increased slightly, by about 30 kg C ha^{-1} yr^{-1} with an increased in annual precipitation by 100 mm, but precipitation hardly influenced other mangrove components for a precipitation range from 1113 to 1966 mm used in this sensitivity analysis.

5.7. Flux and anaerobic oxidation of methane

Ecological drivers can substantially impact CH_4 production and emissions. CH_4 flux increased or decreased by about 1.1 mg CH_4 m^{-2} d^{-1} with an increase or decrease in temperature of 1 °C (Table 3a), decreased by about 0.04 mg m^{-2} d^{-1} with an increment in latitude of 1°. Similarly, P and salinity can substantially impact CH_4 flux in mangrove ecosystems (Figs. 5b and 7), increased with an increase in P and decreased with an increment in salinity. The results from the sensitivity analysis indicated that temperature, geographical location and salinity can influence CH_4 flux. However, we did not find a substantial trend in increase or decrease in CH_4 flux with an increase or decrease in precipitation within simulation precipitation range (1113–1966 mm), which might be related to the hydrological conditions for this study assumed that was as same as those at ENP in Florida.

The CH_4 flux significantly decreased nonlinearly with an increase in sulfate concentration (Fig. 8), and the flux was strongly sensitive to high sulfate concentration in mangrove soils with a response of fourth degree polynomial. Because other ecological factors were constant except for sulfate, the flux was relatively constant when sulfate ≤ 0.8 mol l^{-1}, showed that the sensitivity of the CH_4 efflux was low at low sulfate concentrations. Accordingly, AOM might occur when sulfate > 0.8 mol l^{-1}.

6. Conclusions

MCAT-DNDC is a stable process-based model capable of simulating carbon dynamics among vegetation, soil and water pools within the mangroves. Sensitivity analysis for temperature, precipitation, salinity, phosphorus, latitude and sulfate used as the model inputs showed that C accumulation and consumption in mangrove ecosystems is sensitive to all of these factors in the MCAT-DNDC simulations.

Overlapping effects of multiple factors were considered to assess C dynamics in mangrove ecosystems in the model MCAT-DNDC. The model was effective at considering their influences and interactions; for example, an increase in temperature and decrease in P deficit can increase C sequestration, but mangrove C can decrease with an increase in salt stress and P deficit.

Unfortunately, we didn't have sufficient available hydrological observations from mangroves to evaluate the sensitivity of the C dynamics with respect to the tidal hydrology. It should be analyzed in future because it can affect the C dynamics in mangrove ecosystems (Krauss et al., 2006), especially with respect to DIC, DOC and POC. In addition, hydrology can be regulated by climate change, especially for riverine mangroves where the hydrology is impacted by the freshwater flux in the rivers.

AOM needs more measurement data to evaluate the processes of the production and oxidation of CH_4 at different soil depths to assess the interactions of sulfate, nitrate and nitrite reduction processes.

The disturbance functionality of the model was not assessed because reliable disturbance response information was not available; simulation of these impacts will need to be calibrated and validated as observations become available. Similarly the effects of hydrology, topographical gradient, and soil/sediment texture on C sequestration in mangroves have not been evaluated because of insufficient data for validation. Additional field studies are needed, including data from different mangrove species and geographical locations for biomass, BC, DOC, DIC, POC, and more.

Dedication

We dedicate this paper to remember Dr. Changsheng Li, a former professor of University of New Hampshire, and the pioneer of the DNDC model.

Acknowledgements

We thank Dr. Jordan Barr from South Florida Natural Resource Center for support for this model development. Support for the development of this model was provided through the Sustainable Wetland Adaptation and Mitigation Program supported by the US Agency for International Development, and the Estimating Total Ecosystem Carbon in Blue Carbon and Tropical Peatland Ecosystems supported by the NASA Carbon Monitoring Systems program.

Appendix

Acronyms

Acronym	Explanation
AGB	Aboveground Biomass
AOM	Anaerobic Oxidation of Methane
ANPP	annual Aboveground Net Primary Productivity
BC	Burial Carbon
C	Carbon
DIC	Dissolved Inorganic Carbon

DOC	Dissolved Organic Carbon
DNDC	Denitrification and Decomposition
ENP	Everglades National Park, located in southern Florida, USA
FDNDC	Forest-DNDC
GHG	Greenhous Gas
GPP	Gross Primary Productivity
LAI	Leaf Area Index
LLT	Leaf Litter
LPD	Leaf biomass
MCAT	Mangrove Carbon Assessment Tool
MDT	Mean Daily Temperature
MRV	Monitoring, Reporting and Verification
N	Nitrogen
NEE	Net Ecosystem Exchange
NPP	Net Primary Productivity
P	Phosphorous
PAR	Photosynthetically Active Radiation
POC	Particulate Organic Carbon
PS	Combined impact of Phosphorous and Salinity
REDD +	Reducing Emissions from Deforestation and forest Degradation, plus conserving forests and promoting sustainable forest management
Rh	Heterotrophic soil Respiration
SLW	Specific Leaf Weight
SP	Combined impact of Salinity and Phosphorous
TLT	Total Litter
WT	Water Table level

References

Alongi, D.M., 2008. Mangroves forests: resilience, protection from tsunami, and responses to global climate change. Estuar. Coast Shelf Sci. 76, 1–13.

Alongi, D.M., 2009. The Energetics of Mangrove Forests. Springer printed in USA, ISBN: 978-1-4020-4270-6.

Alongi, D.M., 2014. Carbon cycling and storage in mangrove forests. Ann. Rev Mar. Sci. 6, 195–219.

Atlas, E., Culberson, C., Pytkowicz, R.M., 1976. Phosphate association with Na+, Ca^{2+} and Mg^{2+} in seawater. Mar. Chem. 4, 243–254.

Ball, M.C., Farquhar, G.D., 1984. Photosynthetic and stomatal responses of the grey mangrove, *Avicennia marina*, to transient salinity conditions. Plant Physiol. 74, 7–11.

Ball, M.C., Pidsley, S.M., 1995. Growth responses to salinity in relation to distribution of two mangrove species, Sonneratia alba and S. lanceolata, in northern Austrialia. Funct. Ecol. 9, 77–85.

Barr, J.G., Fuentes, D., O'Halloran, T., Barr, D., Zieman, J.C., Childers, D.L., 2006. Carbon assimilation by mangrove forests in the Florida Everglades. Amalgam 1, 27–37.

Barr, J.G., Engel, V., Fuentes, J.D., Zieman, J.C., O'Halloran, T.L., Simth III, T.J., Anderson, G.H., 2010. Controls on mangrove forest-atmosphere carbon dioxide exchanges in western Everglades National Park. JGR 115http://dx.doi.org/10.1029/2009JG001186. G02020.

Barr, J.G., Engel, V., Smith, T.J., Fuentes, J.D., 2012. Hurricane disturbance and recovery of energy balance, CO_2 fluxes and canopy structure in a mangrove forest of the Florida Everglades. Agric. For. Meteorol. 153, 54–66. http://dx.doi.org/10.1016/j.agfformet.2011.07.022.

Barr, J.G., Engel, V., Fuentes, J.D., Fuller, D.O., Kwon, H., 2013a. Modeling light use efficiency in a subtropical mangrove forest equipped with CO_2 eddy covariance. Biogeosciences 10, 2145–2158. http://dx.doi.org/10.5194/bg-10-2145-2013.

Barr, J.G., Fuentes, J.D., Delonge, M.S., O'Halloran, T.L., Barr, D., Zieman, J.C., 2013b. Summertime influences of tidal energy advection on the surface energy balance in a mangrove forest. Biogeosciences 10, 1–11. http://dx.doi.org/10.5194/bg-10-1-2013.

Baturin, G.N., 2003. Phosphorus cycle in the ocean. Lithol. Miner. Resour. 38, 101–119.

Bolan, N.S., 1991. A critical review on the role of mycorrhizal fungi in the uptake of phosphorus by plants. Plant Soil 134, 189–207.

Bouillon, S., Borges, A.V., Castaneda-Moya, E., Diele, K., Dittmar, T., Duke, N.C., Kristensen, E., Lee, S.Y., Marchand, C., Middelburg, J.J., Rivera-Monroy, V.H., Smith II, T.J., Twilley, R.R., 2008. Mangrove production and carbon sinks: a revision of global budget estimates. Global Biogeochem. Cycles 22http://dx.doi.org/10.1029/2007GB003052. GB2013.

Bridgham, S.D., Updegraff, K., Pastor, J., 1998. Carbon, nitrogen, and phosphorus mineralization in northern wetlands. Ecology 79, 1545–1561.

Bukoski, J.J., Broadhead, J.S., Donato, D.C., Murdiyarso, D., Gregoire, T.G., 2017. PLoS One. http://dx.doi.org/10.1371/joural.pone.0169096.

Burton, E., Walter, L.M., 1990. The role of pH in phosphate inhibition of calcite and aragonite precipitation rates in seawater. Geochem. Cosmochim. Acta 54, 797–808.

Caldwell, S.L., Laidler, J.R., Brewer, E.A., Eberly, J.O., Sandborgh, S.C., Colwell, F.S., 2008. Anaerobic oxidation of methane: mechanisms, bioenergetics, and the ecology of associated microorganisms. Environ. Sci. Technol. 42, 6791–6799.

Chapin III, F.S., 1980. The mineral nutrition of wild plants. Annu. Rev. Ecol. Systemat. 11, 233–260.

Castaneda-Moya, E., Twilley, R.R., Rivera-Monroy, V.H., 2013. Allocation of biomass and net primary productivity of mangrove forests along environmental gradients in the Florida coastal Everglades, USA. For. Ecol. Manag. 307, 226–241.

Chen, R., Twilley, R., 1998. A gap dynamic model of mangrove forest development along gradients of soil salinity and nutrient resources. J. Ecol. 86, 37–51.

Chen, R., Twilley, R.R., 1999. Patterns of mangrove forest structure and soil nutrient dynamics along the Shark River estuary, Florida. Estuaries 22, 955–970.

Clarkson, D.T., 1985. Factors affecting mineral nutrient acquisition by plants. Annu. Rev. Plant Physiol. 36, 77–115.

Clough, B., 1998. Mangrove forest productivity and biomass accumulation in Hinchinbrook Channel, Australia. Mangroves Salt Marshes 2, 191–198.

Cui, J., Li, C., Sun, G., Trettin, C., 2005. Linkage of MIKE SHE to Wetland-DNDC for carbon budgeting and anaerobic biogeochemistry simulation. Biogeochemistry 72, 147–167.

Dai, Z., Trettin, C.C., Li, C., Li, H., Sun, G., Amatya, D.M., 2012. Effect of assessment scale on spatial and temporal variations in CH_4, CO_2 and N_2O fluxes in a forested watershed. Water Air Soil Pollut. 223, 253–265. http://dx.doi.org/10.1007/s11270-011-0855-0.

Dai, Z., Birdsey, R.A., Johnson, K.D., Dupuy, J.M., Hernandez-Stefanoni, J.L., Richardson, K., 2014. Modeling carbon stocks in a secondary tropical dry forest in the Yucatan Peninsula, Mexico. Water Air Soil Pollut. 225, 1925. http://dx.doi.org/10.1007/s11270-014-1925-x.

Dai, Z., Birdsey, R.A., Dugan, A.J., 2017. Estimated carbon sequestration in a temperate forest in Idaho of USA. Nat. Sci. 9, 421–436. http://dx.doi.org/10.4236/ns.2017.912040.

Dakora, F.D., Phillips, D.A., 2002. Root exudates as medistors of mineral acquisition in low-nutrient environments. Plant Soil 245, 35–47.

Day Jr., J.W., Coronado-Molina, C., Vera-Herrera, F.R., Twilley, R., Rivera-Monroy, V.H., Alvarez-Guillen, H., Day, R., Conner, W., 1996. A 7 year record of above-ground net primary production in a southeastern Mexican mangrove forest. Aquat. Bot. 55, 39–60.

Dittmar, T., Hertkorn, N., Kattner, G., Lara, R.J., 2006. Mangroves, a major source of dissolved organic carbon to the oceans. Global Biogeochem. Cycles 20http://dx.doi.org/10.1029/2005GB002570. GB1012.

DOE, 1994. Handbook of methods for the analysis of the various parameters of the carbon dioxide system in sea water, version 2. In: Dickson, A.G., Goyet, G. (Eds.), ORNL/CDIAC-74, (Washington D.C).

Donato, D.C., Kauffman, J.B., Murdiyarso, D., Kurnianto, S., Stidham, M., Kanninen, M., 2011. Mangroves among the most carbon-rich forests in the tropics. Nat. Geosci. 4, 293–297.

Ettwig, K.F., Butler, M.K., Paslier, D.L., Pelletier, E., Mangenot, S., Kuyers, M.M.M., Schreiber, F., Dutilh, B.E., Zedelius, J., Beer, D.D., Gloerich, J., Wessels, H.J.C.T., Alen, T.V., Luesken, F., Wu, M.L., Pas-Schoonen, K.T.V.D., Camp, H.J.M.O.D., Janssen-Megens, E.M., Francoijs, K.J., Stunnenberg, H., Weissenbach, J., Jetten, M.S.M., Strous, M., 2010. Nitrite-driven anaerobic methane oxidation by oxygenic bacteria. Nature 464, 543–548.

FAO, 1994. Mangrove Forest Management Guidelines. FAO Forest Paper 117. FAO Forest Department, Rome, pp. 345.

FAO, 2007. The World's Mangroves 1998 – 2005. A Thematic Study Prepared in the

Framework of Global Forest Resources Assessment, FAO Forest Paper 153. FAO Forestry Department, Rome, pp. 89.
Filippelli, G.M., 1997. Controls on phosphorus concentration and accumulation in oceanic sediments. Mar. Geol. 139, 231–240.
Filippelli, G.M., Delaney, M.L., 1996. Phosphorus geochemistry of equatorial Pacific sediments. Geochem. Cosmochim. Acta 60, 1479–1495.
Follmi, K.B., 1996. The phosphorus cycle, phosphogenesis and marine phosphate-rich deposits. Earth Sci. Rev. 40, 55–124.
Froelich, P.N., 1988. Kinetic control of dissolved phosphate in natural rivers and estuaries: a promer on the phosphate buffer mechanism. Limnol. Oceanogr. 33, 649–667.
Galvan-Ampudia, C.S., Testerink, C., 2011. Salt stress signals shape the plant root. Plant Biol. 14, 296–302.
Grattan, S.R., Grieve, C.M., 1992. Mineral element acquisition and growth response of plant grown in saline environments. Agric. Ecosyst. Environ. 38, 275–300.
Grattan, S.R., Grieve, C.M., 1999. Salinity-mineral nutrient relations in horticultural crops. Sci. Hortic. 78, 127–157.
Green-Saxena, A., Dekas, A.E., Dalleska, N.F., Orphan, V.J., 2014. Nitrate-based niche differentiation by distinct sulfate-reducing bacteria involved in the anaerobic oxidation of methane. ISME J. 8, 150–163.
Grueters, U., Seltmann, T., Schmidt, H., Horn, H., Pranchai, A., Voviders, A.G., Peters, R., Vogt, J., Dahdouh-Guebas, F., Berger, U., 2014. The mangrove forest dynamics model mesoFON. Ecol. Model. 291, 28–41.
Haroon, M.F., Hu, S., Shi, Y., Imelfort, M., Keller, J., Hugenholtz, P., Yuan, Z., Tyson, G.W., 2013. Anaerobic oxidation of methane coupled to nitrate reduction in a novel archaeal lineage. Nature 500, 567–570. http://dx.doi.org/10.1038/nature12375.
Hutchison, J., Manica, A., Swetnam, R., Balmford, A., Spalding, M., 2013. Predicting global patterns in mangrove forest biomass. Conserv. Lett. http://dx.doi.org/10.111/conl.12060.
Ingall, E.D., Bustin, R.M., Cappellen, P.V., 1993. Influence of water column anoxia on the burial and preservation of carbon and phosphorus in marine shales. Geochem. Cosmochim. Acta 57, 303–316.
Jardine, S.L., Siikamaki, J.V., 2014. A global predictive model carbon in mangrove soils. Environ. Res. Lett. 9. http://dx.doi.org/10.1088/1748-9326/10/104013.
Jennerjahn, T.C., Gilman, E., Krauss, K.W., lacerda, L.D., Nordhaus, I., Wolanski, E., 2017. Mangrove ecosystems under climate change. In: Rivera-Monroy, V.H., Lee, S.Y., Kristensen, E., Twilley, R.R. (Eds.), Mangrove Ecosystems: a Global Biogeographic Perspective. Springer, Cham Online ISBN: 978-3-319-62206-4. https://doi.org/10.1007/978-3-319-62206-4.
Johansson, O., Wedborg, M., 1979. Stability constants oh phosphoruric acid in seawater of 5-40% salinity and temperatures of 5-25°C. Mar. Chem. 8, 57–69.
Jones, T.G., Rakoto Ratsimba, H., Ravaoarinorotsihoarana, L., Cripps, G., Bey, A., 2014. Ecological variability and carbon stock estimates of mangrove ecosystems in northwestern Madagascar. Forests 5, 177–205. http://dx.doi.org/10.3390/f5010177.
Joye, S.B., Boetius, A., Orcutt, B.N., Montoya, J.P., Schulz, H.N., Erickson, M.J., Lugo, S.K., 2004. The anaerobic oxidation of methane and sulfate reduction in sediments from Gulf of Mexico cold seeps. Chem. Geol. 205, 210–238.
Joye, S.B., 2012. A piece of the methane puzzle. Nature 491, 538–539.
Kathiresan, K., Rajendran, N., 2005. Coastal mangrove forests mitigated tsunami. Estuar. Coast Shelf Sci. 65, 601–606.
Kauffman, J.B., Heider, C., Cole, T.G., Dwire, K.A., Donato, D.C., 2011. Ecosystem carbon stocks of Micronesian mangrove forests. Wetlands 31, 343–352. http://dx.doi.org/10.1007/s13157-011-0148-9.
Kauffman, J.B., Heider, C., Norfolk, J., Payton, F., 2014. Carbon stocks of intact mangroves and carbon emissions arising from their conversion in the Dominican Republic. Ecol. Appl. 24, 518–527.
Kirschbaum, M.U.F., Gifford, R.M., Roxburgh, S.H., Sands, P.J., 2001. Definitions of some ecological terms commonly used in carbon accounting. In: Kirschbaum, M.U.F., Mueller, R. (Eds.), Proceedings: Net Ecosystem Exchange. Cooperative Research Centre for Greenhouse Accounting, pp. 18–20 April 2001, Commonwealth of Australia.
Krauss, K.W., Doyle, T.W., Twilley, R.R., Rivera-Monroy, V.H., Sullivan, J.K., 2006. Evaluating the relative contributions of hydroperiod and fertility on growth of south Florida mangroves. Hydrobiologia 569, 311–324.
Li, C., Frolking, S., Frolking, T.A., 1992. A model of nitrous oxide evolution from soil driven by rainfall events: 1. Model structure and sensitivity. JGR 97, 9759–9776.
Li, C., Aber, J., Stang, F., Butter-Bahl, K., Papen, H., 2000. A process-oriented model of N_2O and NO emissions from forest soils. 1. Model development. J. Geoph. Res. Atmos. 105, 4369–4384.
Li, C., Cui, J., Sun, G., Trettin, C.C., 2004. Modeling impacts of management on carbon sequestration and trace gas emissions in forested wetland ecosystems. Environ. Manag. 33, S176–S186.
Li, C., 2007. Quantifying greenhouse gas emissions from soils: scientific basis and modeling approach. Soil Sci. Plant Nutr. 53, 344–352.
Liang, S., Zhou, R., Dong, S., Shi, S., 2008. Adaptation to salinity in mangroves: implication on the evolution of salt-tolerance. Chin. Sci. Bull. 53, 1708–1715.
Lin, G., Sternberg, L.S.L., 1992. Effect of growth form, salinity, nutrient and sulfide on photosynthesis, carbon isotope discrimination and growth of red mangrove (*Rhizophora mangle* L.). Aust. J. Plant Physiol. 19, 509–517.
Lovett, G.M., Cole, J.J., Pace, M.L., 2006. Is net ecosystem production equal to ecosystem carbon accumulation? Ecosystems 9, 1–4. http://dx.doi.org/10.1007/s10021-005-0036-3.
Luo, Z., Sun, O.J., Wang, E., Ren, H., Xu, H., 2010. Modeling productivity in mangrove forests as impacted by effective soil water availability and its sensitivity to climate change using Biome-BGC. Ecosystems 13, 949–965. http://dx.doi.org/10.1007/s10021-010-9365-y.
Matsui, N., 1998. Estimated stocks of organic carbon in mangrove roots and sediments in Hinchinbrook Channel, Australia. Mangroves Salt Marshes 2, 199–204.
Miehle, P., Livesley, S.J., Feikema, P.M., Li, C., Arndt, S.K., 2006. Assessing productivity and carbon sequestration capacity of Eucalyptus globules plantation using the process model Forest-DNDC: calibration and validation. Ecol. Model. 192, 83–94.
Milucka, J., Ferdelman, T.G., Polerecky, L., Frankzke, D., Wegener, G., Schmid, M., Lieberwirth, I., Wagner, M., Widdel, F., Kuypers, M.M., 2012. Zero-valent Sulphur is a key intermediate in marine methane oxidation. Nature 491, 541–546. http://dx.doi.org/10.1038/nature11656.
Mukherjee, N., Sutherland, W.J., Khan, M.N.I., Berger, U., Schmitz, N., Dahdouh-Guebas, F., Koedam, N., 2014. Using expert knowledge and modeling to define mangrove composition, functioning, and threats and estimate time frame for recovery. Ecol. Evol. 4, 2247–2262. http://dx.doi.org/10.1002/ece3.1085.
Naidoo, G., 1987. Effects of salinity and nitrogen on growth and water relations in the mangrove, *Avicennia marina* (Forsk.) Vierh. New Phytol. 107, 317–325.
Nguyen, H.T., Stanton, D.E., Schmitz, N., Farquhar, G.D., Ball, M.C., 2015. Growth responses of the mangrove Avicennia marina to salinity: development and function of shoot hydraulic systems require saline conditions. Ann. Bot. 115, 397–407.
Osland, M.J., Enwright, N., Stagg, C.L., 2014. Freshwater availability and coastal wetland foundation species: ecological transitions along a rainfall gradient. Ecology 95, 2789–2802.
Parida, A.K., Das, A.B., Mittra, B., 2004. Effects of salt on growth, ion accumulation, photosynthesis and leaf anatomy of the mangrove, Bruguiera parviflora. Trees 18, 167–174. http://dx.doi.org/10.1007./s00468-003-0293-8.
Parida, A.K., Das, A.B., 2005. Salt tolerance and salinity effects on plants: a review. Ecotoxicol. Environ. Saf. 60, 324–349.
Raghoebarsing, A.A., Pol, A., Pas-Schoonen, K.T.V.D., Smolders, A.J.P., Ettwig, K.F., Rijpstra, W.I.C., Schouten, S., Sinninghe Damste, J.S., Camp, H.J.M.O.D., Jetten, M.S.M., Strous, M., 2006. A microbial consortium couples anaerobic methane oxidation to denitrification. Nature 440, 918–921.
Rahman, M.M., Khan, M.N.I., Hoque, A.K.F., Ahmed, I., 2015. Carbon stock in the Sundarbans mangrove forests: spatial variations in vegetation types and salinity zones. Wetl. Ecol. Manag. 23, 269–283.
Raymond, P.A., Bauer, J.E., Cole, J.J., 2000. Atmospheric CO_2 evasion, dissolved inorganic carbon production, and net heterotrophy in the York River estuary. Limol. Oceanogr. 45, 1707–1717.
Rideout, A.J.R., Josh, N.P., Viergever, K.M., Huxham, M., Briers, R.A., 2013. Making predictions of mangrove deforestation: a comparison of two methods in Kenya. Global Change Biol. 19, 3493–3501. http://dx.doi.org/10.111/gcb.12176.
Romigh, M.M., Davis II, S.E., Rivera-Monroy, V.H., Twilley, R.R., 2006. Flux of organic carbon in a riverine mangrove wetland in the Florida Coastal Everglades. Hydrobiologia 569, 505–516. http://dx.doi.org/10.1007/s10750-006-0152-x.
Schachtman, D.P., Reid, R.J., Ayling, S.M., 1998. Phosphorus uptake by plants: from soil to cell. Plant Physiol. 116, 447–453.
Shima, S., Thauer, R.K., 2005. Methyl-coenzyme M reductase and the anaerobic oxidation of methane in methanotrophic Archaea. Curr. Opin. Microbiol. 8, 643–648.
Stange, F., Butterbachl, K., Papen, H., Zechmeister-Boltenstern, S., Li, C., Aber, J., 2000. A process-oriented model of N_2O and NO emissions from forest soils. J. Geophys. Res. 105, 4385–4398.
Suarez, N., Medina, E., 2005. Salinity effect on plant growth and leaf demography of mangrove, *Avicennia germinans* L. Trees 19, 721–727.
Sun, R., Duan, Z., 2007. An accurate model to predict the thermodynamic stability of methane hydrate and methane solubility in marine environments. Chem. Geol. 244, 248–262.
Takemura, T., Hanagata, N., Sugihara, K., Baba, S., Karube, I., Dubinsky, Z., 2000. Physiological and biochemical responses to salt stress in the mangrove, Bruguera gymnorrhiza. Aquat. Bot. 68, 15–28.
Thauer, R.K., 2011. Anaerobic oxidation of methane with sulfate: on the reversibility of the reactions that are catalyzed by enzymes also involved in methanogenesis from CO_2. Curr. Opin. Microbiol. 14, 292–299.
Thornton, P.E., Thornton, M.M., Mayer, B.W., Wilhelmi, N., Wei, Y., Cook, R.B., 2012. Daymet: Daily Surface Weather on a 1 Km Grid for North America, 1980-2008. http://dx.doi.org/10.3334/ORNLDAAC/Daymet_V2. Acquired online. http://daymet.ornl.gov/ on 30/08/2014 from Oak Ridge National Laboratory Distributed Active Archive Center, Oak Ridge, Tennessee, U.S.A.
Tiessen, H., Stewart, J.W.B., Cole, C.V., 1984. Pathways of phosphorus transformations in soils of differing pedogenesis. Soil Sci. Soc. Am. J. 48, 853–858.
Twilley, R.R., 1985. The exchange of organic carbon in basin mangrove forests in a southwest Florida estuary. Estuar. Coast Shelf Sci. 20, 543–557.
Twilley, R.R., Day Jr., J.W., 1999. The productivity and nutrient cycling og mangrove ecosystems. In: Yanez-Arancibia, A., Lara-Dominguez, A.L. (Eds.), Ecosistemas de manglar en America Tropical. Instituto de Ecologia A.C. Mexico, UICN/ORMA, Costa Rica, NOAA/NMFS Silver Spring MD USA 380pp.
Van der Molen, D.T., 1991. A simple, dynamic model for the simulation of the release of phosphorus from sediments in shallow, eutrophic systems. Water Res. 25, 737–744.
Vazquez, P., Holguin, G., Puente, M.E., Lopez-Cortes, A., Bashan, Y., 2000. Phosphate-solubilizing microorganisms associated with the rhizosphere of mangroves in a semiarid coastal lagoon. Biol. Fertil. Soils 30, 460–468.
Wang, G., Guan, D., Peart, M.R., Chen, Y., Peng, Y., 2013. Ecosystem carbon stocks of mangrove forest in Yingluo Bay, Guangdong province of south China. For. Ecol. Manag. 310, 539–546.
Zhang, Y., Li, C., Trettin, C.C., Li, H., Sun, G., 2002. An integrated model of soil, hydrology, and vegetation for carbon dynamics in wetland systems. Global Biogeochem. Cycles 16http://dx.doi.org/10.1029/2001GB001838. GB001838.